Hindawi
Advances in Civil Engineering
Volume 2022, Article ID 4691972, 16 pages
https://doi.org/10.1155/2022/4691972

Research Article

Mechanical and Durability Performance of High-Strength Concrete with Waste Tyre Steel Fibres

Daudi Salezi Augustino,[1] **Richard Ocharo Onchiri**,[2] **Charles Kabubo**,[3] **and Christopher Kanali**[4]

[1]*Pan-African University, Institute for Basic Sciences, Technology and Innovation Hosted at Jomo Kenyatta University of Agriculture and Technology (JKUAT), Nairobi, Kenya*
[2]*Department of Building and Civil Engineering, Technical University of Mombasa (TUM), Mombasa, Kenya*
[3]*Department of Civil, Construction and Environmental Engineering, Jomo Kenyatta University of Agriculture and Technology (JKUAT), Nairobi, Kenya*
[4]*Department of Agricultural and Biosystems Engineering, Jomo Kenyatta University of Agriculture and Technology (JKUAT), Nairobi, Kenya*

Correspondence should be addressed to Daudi Salezi Augustino; daudiaugustino974@yahoo.com

Received 12 March 2022; Revised 3 May 2022; Accepted 25 May 2022; Published 20 June 2022

Academic Editor: Yiwei Weng

Concrete with various fibres has been in practice over the years now to improve the internal characteristics of concrete. In most of the developing countries, there is a high rate of waste tyres due to the importation of used cars. Waste tyres increase the environmental burden due to their resistance to decomposition in landfills. To have alternative disposal of waste tyres, their components of steel fibres were utilized in concrete to assess their effect on the mechanical and durability performance of high-strength concrete with a target mean strength of 70 MPa. Fibres had a diameter of 1.3 mm and lengths of 30, 50, and 60 mm with fibre contents of 0.3, 0.5, 0.75, and 1.0% in each length. Slump tests were performed on fresh concrete with and without fibres. The mechanical performance variables assessed were compressive strength, splitting tensile strength, flexural strength, flexural toughness, residual strength, static modulus, and Poisson's ratio. In addition, durability tests such as chloride ion penetration and absorption rate of water were investigated. The results showed that an increase in fibre length to 60 mm and a 1.0% fibre content resulted in the high bond strength in the concrete matrix resulting in a smaller crack width. Moreover, these fibre length and content resulted in improved tensile and flexural strength to 21.5% and 71.1% of control mix, respectively. The increase in fibre length and content affected both the durability properties and the flowability of the concrete, and as for length (60 mm) and 1% content, concrete had a slump of 77.8% lesser compared to the control mix. The compressive strength was improved to 15.2% for concrete with a fibre length of 50 mm and a fibre content of 0.5%. However, further increases in fibre content and length caused an increase in the number of weaker interfacial transition zones at the composite interface that reduces compressive stiffness, resulting in low compressive strength. Furthermore, the reduced fibre content and length (30 mm) improve the static modulus linearly up to 0.75% fibre content; however, concrete with a fibre length of 50 mm and content of 0.3% gives the best results.

1. Introduction

Fibre-reinforced concrete has been used in the building industry over the years, particularly when structural engineers require the initial improvement of the mechanical properties of concrete. In most developing countries, there is a high rate of waste tyres due to the importation of used cars. The waste tyres increase the burden on the environment because they are resistant to degradation in landfills. According to National Transport Service Authority in Kenya, 90,000 vehicles were registered in 2019 with a forecast of 1.35 million vehicles in 2030. These cars produce

several sets of waste tyres during a lifetime, increasing the demand for their reuse. To develop an effective alternative for the disposal of waste tyres in East African cities while improving the properties of concrete composites, the reuse of steel fibres from the pyrolysis process of used car tyres is the paramount aspect to investigate. Past studies have investigated the importance of reusing rubber in cementitious composites such as blocks and concrete as recyclability practices of the waste tyre [1, 2]. However, in these studies and in many pyrolysis processes, less emphasis is placed on how to protect the environment against residual steel fibres. Fibre-reinforced concrete is required in infrastructures where electromagnetic neutrality is required and where lightweight structures are required [3]. Along with the use of fibres in concrete, the sustainable use of natural resources needs an emphasis. The application of aggregates in the construction industry can be minimized by reducing the size of structural elements. This is achieved by adopting high-strength concrete. An increase in the concrete grade of more than 50 MPa results in a concrete with less ductility, which is prone to failure in tensile load configurations.

The ductility in the structure can significantly resist the devastating failure under seismic load, provide a warning before the failure of the structures, and delay the formation of rapid plasticity in structural elements such as beams [4, 5]. The ductility of high-strength concrete can be improved by incorporating fibres into the matrix. Concrete with high fibre content has a high dynamic increase factor and general dynamic responses, resulting in high resistance to structural failure under dynamic excitation [6]. Several studies agree that the inclusion of straight fibres in concrete improves its tensile and flexural strength under monolithic loading. However, this has less influence on shear resistance and compressive strength of concrete with fibre content more than 1.0% [7, 8]. The reduction in compressive strength is associated with the excessive congestion of the fibres in the matrix, leading to less binder across the fibres resulting in weak zones and low bonds in the matrix [9]. Compressive strength is a key aspect of shear transfer in a concrete section. Therefore, a low compressive resistance could lead to a weak fibre-concrete interface that could affect the shear transfer mechanism of the fibre. Fibre in concrete matrix under shear transfers shear in terms of compressive strain [10]. Despite the shear transfer by fibre, the inclusion of fibres improves the load-carrying capacity after first crack (strain hardening). The study by [11] concluded that fibre content between 0 and 3% increases the flexural strength by 244%. This increase advances the postbehaviour of fibre-reinforced concrete to carry more loads.

To facilitate load transfer in concrete, the shape and surface texture of the fibres play an important role. For instance, the hooked-end fibres offer high resistance to concrete pullout under tension. Previous studies [12, 13] hypothesized that hook fibres have high contact pressure in the localized area of the hook compared to straight steel fibres. This pressure leads to high friction stresses when the matrix is loaded that contribute to the bond strength of the matrix at the initial damage/cracking of fibre-concrete interface. Despite that hooked steel fibres are the best for improving mechanical properties up to 1.5% fibre content, most of these are synthetic/industrial fibres that are economically unviable in the construction industry compared to straight waste tyre steel fibres. According to [14], concrete with a 1% content of industrial fibres increases the cost of production and increases carbon emissions to about 84.4% and 58%, respectively.

High-strength concrete has a dense matrix that improves its performance in terms of durability compared to normal concrete [15, 16]. However, the inclusion of fibres can trigger this performance in the area with high humidity and high concentration of chloride ions. Due to the variability of steel fibres in tyres, the extent of their performance in concrete has not been well established. To date, research on the mechanical properties of concrete has mostly focused on the utilization of industrial steel fibres. However, the field of durability and mechanical performance of composites with waste tyre steel fibres is drawing growing attention due to the environmental demand for these wastes and the required ductility of HSC. Therefore, this work aims to broaden the understanding of the effects of waste tyre fibres on Poisson's ratio, the ingress of harmful chemicals, sorptivity, and the mechanical properties of high-strength concrete (HSC).

2. Materials and Methods

2.1. Materials. Bamburi Portland cement CEM I 42.5 was used in this study as per EN197-1 [17]. The coarse and fine aggregates were sourced from Mlolongo quarries in Nairobi, Kenya. The coarse aggregates had a maximum size of 12.5 mm. To maintain the flowability of the concrete matrix, Sika Viscocrete 3088 superplasticiser was also used. This superplasticiser type is a high-range water-reducing admixture (HRWRA). It has a density of 1.05 kg/litre and a pH of 4.5 ± 0.5 according to the manufacturer product data sheet. The steel fibres that were used in this study were processed by pyrolysis in a plant in the Athi River area, Machakos County, Kenya. A summary of the materials used in the study is presented in Table 1.

2.1.1. Characterization of Aggregates. The coarse aggregates were sieved and graded according to ASTM 33 [18]. Relative densities of aggregates were determined as per BS 812 [19]. The determination of relative densities for fine and coarse aggregates involved some steps, such as weighing the mass of the pycnometer with sand- and air-drying of coarse aggregates, as shown in Figures 1(a) and 1(b), respectively.

The fineness modulus of the coarse and fine aggregates was 2.5 and 2.4, falling within the acceptable range of 2.4 to 3.1 for the aggregates to be accepted for concrete production. The grading curves of the aggregates are shown in Figure 2.

2.1.2. Physical and Mechanical Properties of Aggregates. The results of the physical and mechanical properties of the aggregates used in this study are shown in Table 2. Coarse aggregates and fine aggregates with dry-bulk density rolls of 1642 kg/m^3 and 1516 kg/m^3 were used. The coarse aggregates had an aggregate impact value (AIV) and an aggregate

Table 1: Summary of materials used in the study.

Materials	
Cement	CEMI-42.5
Coarse aggregate	Maximum size of 12.5 mm
Superplasticiser	Density of 1.05 kg/litre
Fine aggregate	River sand
Waste tyre steel fibre	Twisted with spiral grip

crushing value (ACV) of 6.2% and 18.2%, less than 10% and 30%, respectively, according to the CML [20].

2.1.3. Characterization of Waste Tyre Fibres. The waste tyre steel fibres were cut into lengths measuring 30, 50, and 60 mm using a bolt clipper. An effective fibre length of 200 mm was used to determine the tensile strength and elongation of the steel fibres using the Hounsfield tensometer as shown in Figure 3(a). Due to the contamination of oil and black carbon in the burning process of tyres, the fibres were washed and dried before they were added to concrete.

2.1.4. Physical and Mechanical Properties of Waste Tyre Steel Fibres. The fibre characterization was performed, and the properties are shown in Table 3. The fibre cord had twenty-seven tiny fibres in it. The fibre had a tensile force and elongation of 901 N and 8 mm, respectively. The average tensile strength of the fibres is consistent with ASTM A820 [21]. Virgin tyre steel cord with a diameter greater than 1.3 mm has a tensile force greater than 1000 N [22]. The small tensile force of the fibre in this study is associated with the high temperature (750°C) used in the tyre burning process. At this temperature, there are microstructural changes in the fibre that result in new sets of defective threads, making it easy for these fibres to break [23, 24].

2.2. Concrete Mixing Proportions and Testing Methods

2.2.1. Mixing Proportions. The target mean compressive strength was 70 MPa. The mix proportions were prepared according to ACI 211 [25], in which the water-to-cement ratio of 0.36 was adopted. To increase workability, a superplasticiser dosage of 0.9% of the weight of cement was used in each mix proportion as more dosage of 1.2% can compromise the properties of concrete [26, 27]. For each length of fibres, the study adopted four different contents as percentages of the density of steel (i.e., 7850 kg/m^3 based on literature). The percentages of fibres with respect to their weight in a cubic metre of concrete and the proportions of the mix are given in Tables 4 and 5, respectively.

2.3. Testing

2.3.1. Compressive Strength Test and Workability. After classification of the materials, concrete cubes measuring 100 × 100 × 100 mm were cast and cured in water for 3, 7, and 28 days for the control mix and 12 sets of specimens with fibres. In each period of curing, three cubes were tested. The workability of concrete in each mix was assessed using a slump cone of 300 mm high in which a slump ruler was used to quantify the slump value as shown in Figure 4. The compressive test was carried out using a universal tensile machine with a capacity of 1500 kN at a load rate of 0.5 kN/s according to EN 12390-3 [28]. The average of three cubes determined the crushing strength of the concrete. Before testing for each period, the concrete cubes were air-dried for one hour to dry the surfaces.

2.3.2. Splitting Tensile Strength Test. To determine the splitting tensile strength, thirteen sets of specimens, namely, control mix, and twelve sets with fibres were considered. Three concrete cylinders were cast and tested for each set on the 28 curing days. The cylinder mould used had diameter of 100 mm and a height of 200 mm. Splitting tensile strength of concrete was performed using the universal tensile machine (UTM), according to EN 12390-6 [29]. The concrete cylinder was placed in the UTM centred between loading plates with a loading rate of 0.1 kN/s until the failure of the specimen.

2.3.3. Flexural Strength Test. The test was carried out using thirteen sets of specimens, namely, control mix and twelve sets with fibres. In each set, three concrete beams with dimensions 150 × 150 × 500 mm were cast and tested for 28 days to determine the flexural strength of high-strength concrete. The test setup was in accordance with ASTM C1018 [30], in which a four-point load system was adopted. A hydraulic jack and load cell of capacities 40 tons and 500 kN, respectively, were used to determine the maximum flexural load. To monitor the deflection, a 20 mm dial gauge was mounted as shown in Figure 5. Load cell and dial gauge were all connected to a data logger in which calibration of load cell and dial gauge was performed before applying jack loads. An average of the three beams determined the flexural strength. Also, the flexural toughness and residual strength at l/150 were evaluated as described in ASTM C1609 [31].

2.3.4. Static Modulus and Poisson's Ratio. In order to determine the static modulus and Poisson's ratio, thirteen sets of specimens, namely, control mix and twelve sets with fibres were considered. Three concrete cylinders were cast and tested for each set on 28 curing days. A 100 mm diameter and 200 mm high cylinder mould was used in the test setup. Two bonded strain gauges, each placed parallel to the axis (both vertical and horizontal axis) and circumferentially mounted at diametrically opposite gauge lines at the mid-height of the concrete cylinder as shown in Figure 6, were used. Each concrete cylinder was set in compression, and these four strain gauges were connected to a data logger. Both the modulus of elasticity and Poisson's ratio were computed based on the working stress of 40% of the ultimate crushing strength of the concrete cylinder as per ASTM C469 [32].

(a) (b)

Figure 1: Determination of relative densities of aggregates. (a) Mass of pycnometer with sand. (b) Drying of coarse aggregates.

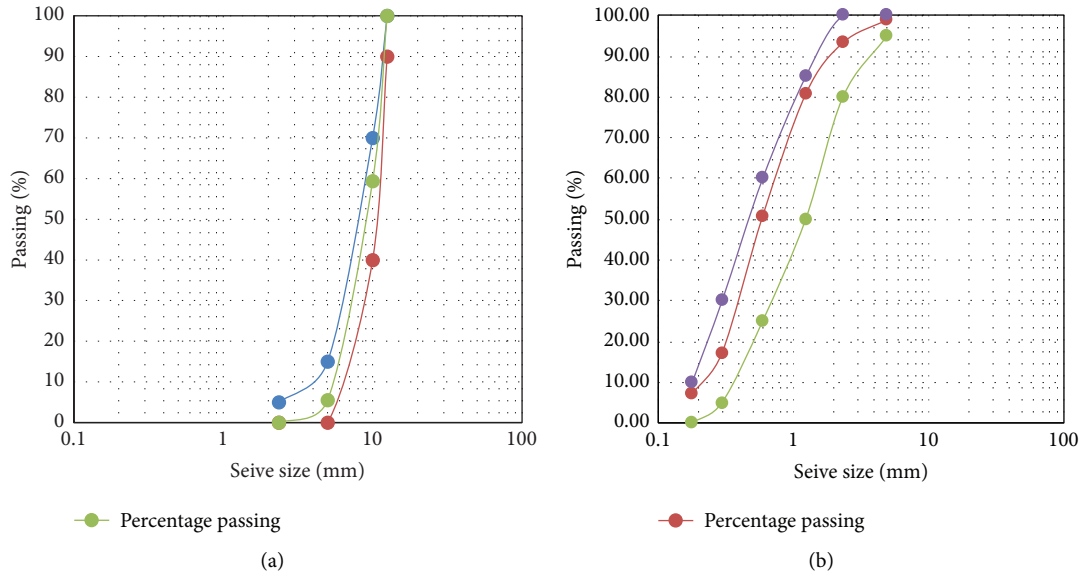

Figure 2: Particle size distribution of aggregates. (a) Coarse aggregates (ballast). (b) Fine aggregates (river sand).

Table 2: Physical and mechanical properties of aggregates.

Properties	Coarse aggregates	Fine aggregates
Relative density on an oven-dry basis	2.44	2.39
Apparent relative density on an oven-dry basis	2.68	2.61
Water absorption (%)	3.6	3.5
Bulk density-dry rolled (Kg/m^3)	1516	1642
Fineness modulus	2.35	2.5
ACV (%)	18.2	—
AIV (%)	6.2	—

2.3.5. Durability Tests

(1) Sorptivity. The test was carried out using thirteen sets of specimens, namely, control mix and twelve sets with fibres. In each set, three cubes measuring $100 \times 100 \times 100$ mm were tested at 28 curing days to assess the absorption rate. Before the test setup, three cubes in each set were baked in the oven for 24 hours. The oven-dried and cooled samples were covered with a plastic sheet on the top and sealed on all sides. These samples were placed in the container with water to allow only the bottom side of the concrete to be in contact with water. The samples were removed from the container and weighed, and the values were recorded at intervals as described in ASTM C1585 [33].

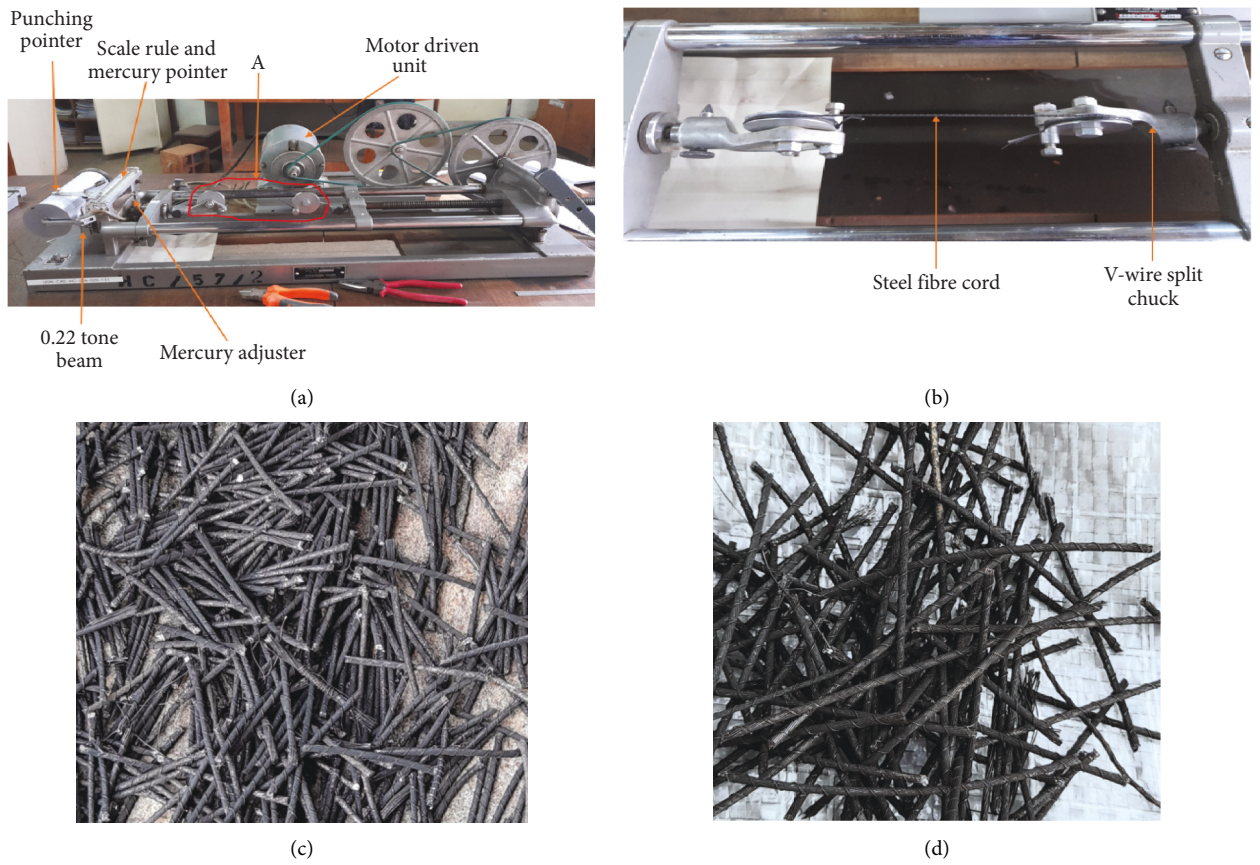

Figure 3: Characterization of waste tyre fibre. (a) Tensile test setup. (b) Region *A*. (c) 30 mm fibre length. (d) 50 mm fibre length.

Table 3: Physical and mechanical properties of waste tyre steel fibres.

Properties	
Diameter-twisted fibre (mm)	1.3
Diameter-individual tiny fibre (mm)	0.3
Cross-sectional area (mm^2)	1.33
Lengths (mm)	30,50,60
Aspect ratios	23,38,46
Tensile force (N)	901
Strain	0.0035
Tensile strength (MPa)	677.4
Elastic modulus (GPa)	193.5
Surface texture	Rough
Shape	Twisted cylindrical

Table 4: Quantity of fibre per 1 m^3 of concrete.

Fibre content (%)	Mass of fibre per cubic metre of concrete (kg/m^3)
0.3	23.55
0.5	39.55
0.75	58.88
1.0	78.5

(2) Chloride Ion Penetration. Twelve sets of concrete with fibres and control mix were used to assess the depth of chloride ions. In each set, three concrete cylinders measuring 100 mm diameter and 200 mm high were cast and cured for 28 days. The samples were then cured in sodium chloride (NaCl) solution for another 28 and 56 days. The curing solution of NaCl contained 3 g of NaCl in 100 ml of water. After curing in NaCl solution, 0.1 M silver nitrate ($AgNO_3$) equivalent to 1.691 g in 100 ml of water was prepared and spread on the separated faces of the concrete cylinder according to ASTM C1543 [34]. The depth of penetration of chloride ions was measured when the colour changed to a white precipitate of silver chloride because of the presence of free chlorides that react with silver nitrate and brown precipitates of silver oxide in the section with no chloride ions. The white colour was recorded as the depth of penetration of chloride ions at an average of 10–20 mm intervals along the length of the cylinder. The preparation of the solution and the split of the cylinders with a change in colour are shown in Figure 7.

3. Results and Discussion

3.1. Workability of Concrete. Figure 8 shows the plot of slump versus various fibre contents with the respective fibre lengths. The control mix had a slump of 90 mm after adding the superplasticiser. The slump value decreases as the content and length of fibres increase. Concrete with the labels SFRC60-0.5, SFRC50-0.5, and SFRC30-0.5 had slump values of 60, 63, and 70 mm and were 33%, 30%, and 22%,

Table 5: Concrete design mix (kg/m^3).

Description	CA*	FA**	C***	W****	Fibre
Mix design	1030.9	676.3	500	180	—
CM[a]	66.98	43.97	32.49	11.7	0
SFRC30-0.3[b]	66.98	43.97	32.49	11.7	1.53
SFRC30-0.5	66.98	43.97	32.49	11.7	2.55
SFRC30-0.75	66.98	43.97	32.49	11.7	3.83
SFRC30-1.0	66.98	43.97	32.49	11.7	5.1
SFRC50-0.3	66.98	43.97	32.49	11.7	1.53
SFRC50-0.5	66.98	43.97	32.49	11.7	2.55
SFRC50-0.75	66.98	43.97	32.49	11.7	3.83
SFRC50-1.0	66.98	43.97	32.49	11.7	5.1
SFRC60-0.3	66.98	43.97	32.49	11.7	1.53
SFRC60-0.5	66.98	43.97	32.49	11.7	2.55
SFRC60-0.75	66.98	43.97	32.49	11.7	3.83
SFRC60-1.0	66.98	43.97	32.49	11.7	5.1

*Coarse aggregate, **fine aggregates, ***cement, ****water, [a]control mix, and [b]steel fibre-reinforced concrete (30 mm fibre length and 0.3% fibre content).

(a) (b)

Figure 4: Concrete workability. (a) 90-mm slump for CM. (b) 20 mm slump for SFRC60-1.0.

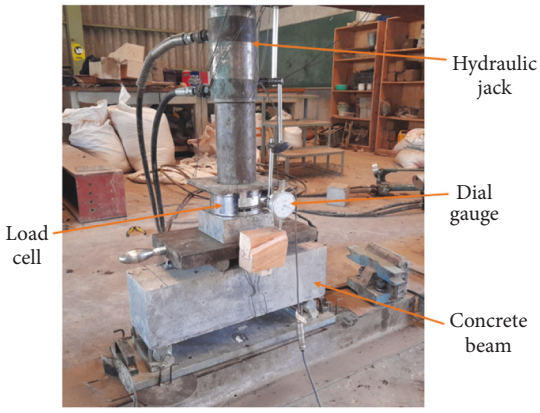

Figure 5: Flexural strength test.

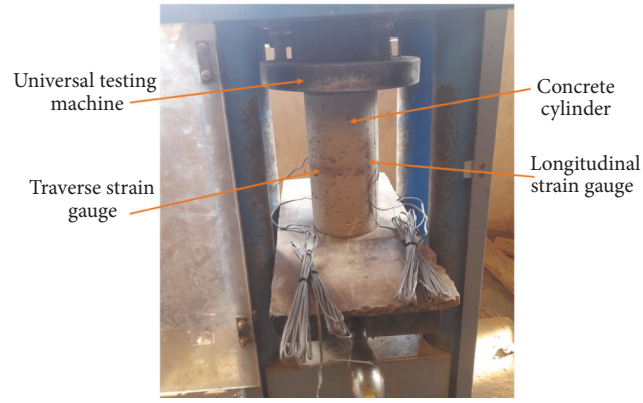

Figure 6: Test setup determination of static Young's modulus and Poisson's ratio of concrete.

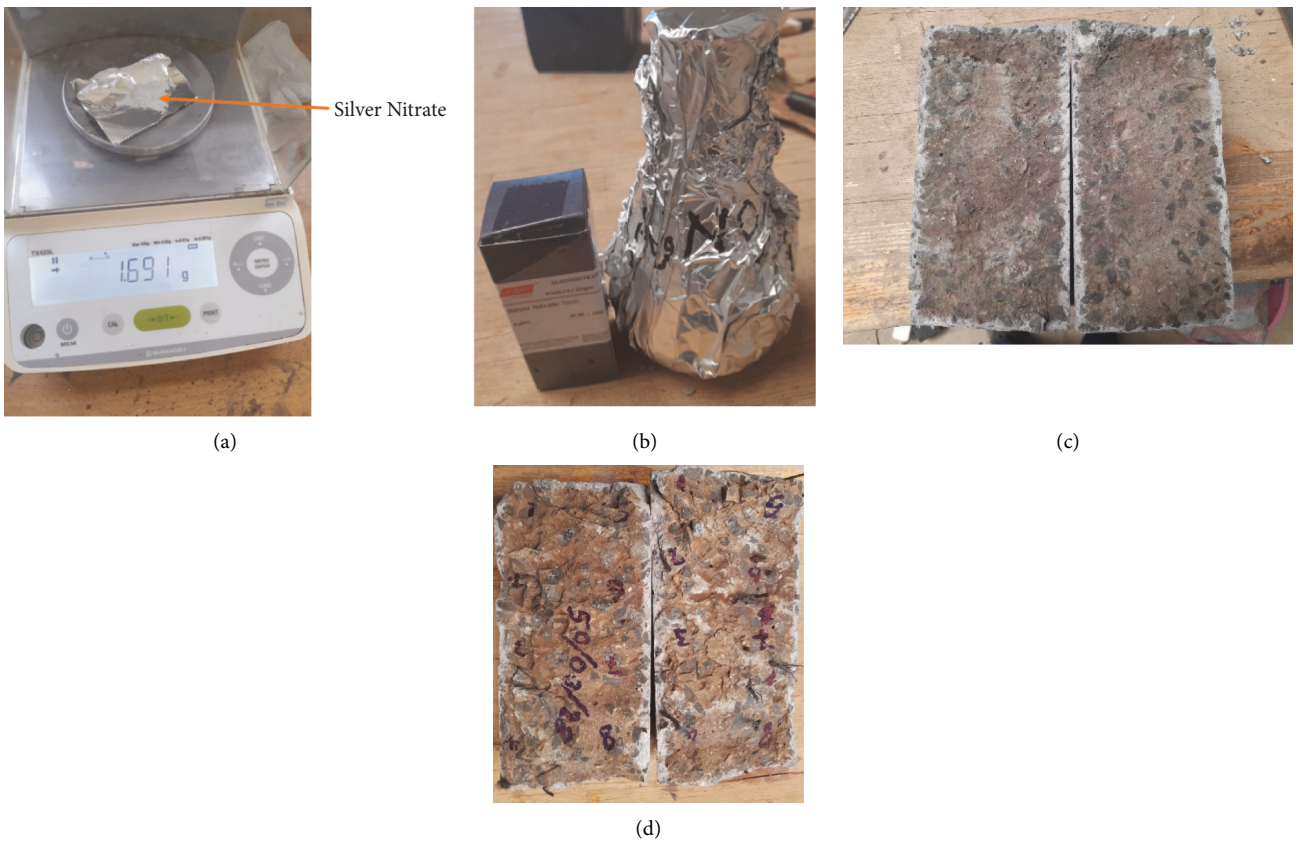

Figure 7: Chloride ion penetration. (a) Weighed silver nitrate powder. (b) 0.1 M silver nitrate solution. (c) Chloride ion penetration depth for CM after curing for 28 days in NaCl solution. (d) Chloride ion penetration depth for SFRC30-0.75 after curing for 28 days in NaCl solution.

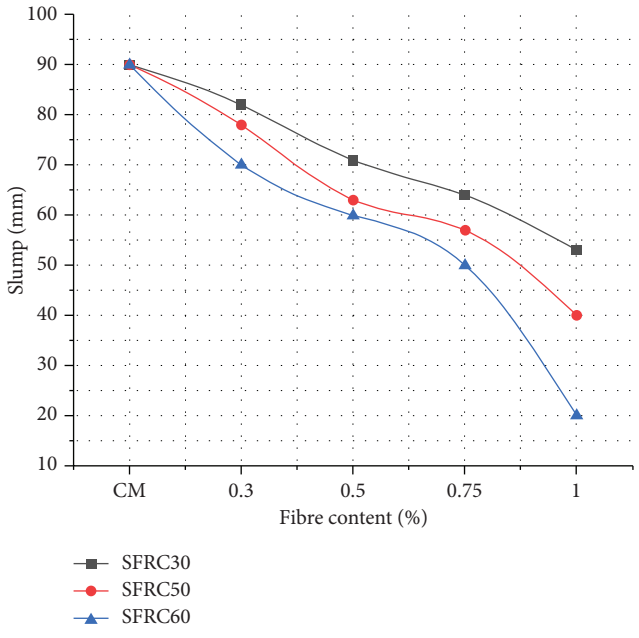

Figure 8: Effect of fibres on the workability performance of high-strength concrete.

respectively, less than the control mix. Moreover, for the same length, SFRC60-0.3, SFRC60-0.5, SFRC60-0.75, and SFRC60-1.0 had slump values of 70, 60, 50, and 20 mm, respectively. This study confirms previous studies by [35, 36] that the workability performance of high-strength concrete is affected by increasing the volume of fibre in it. Increased length and content increase the blockage of concrete ingredients and lead to an increase in the surface area of the mix. This surface area increases the requirements for admixtures and water for both workability and hydration, respectively.

3.2. Mechanical Properties of Concrete

3.2.1. Compressive Strength. The results of compressive strength against curing age and fibre content are plotted in Figure 9. The results of this study are consistent with earlier literature studies. Compressive strength is affected by curing age, and it increases as curing age increases. The control mix showed less compressive strength compared to the concrete with fibres. The results showed that the compression strength increases for low fibre content due to the best attachment at the fibre-concrete interface. Concrete with medium fibre length of 50 mm and 0.5% fibre content had 15.2% increase in compressive strength than the control mix. The failure mode was brittle for the control mix, compared to the reinforced fibre-concrete cubes that failed with relatively little brittleness. Concrete with fibres has an embedment length that increases the strength of the matrix through friction between the fibre and the concrete surfaces that improves resistance

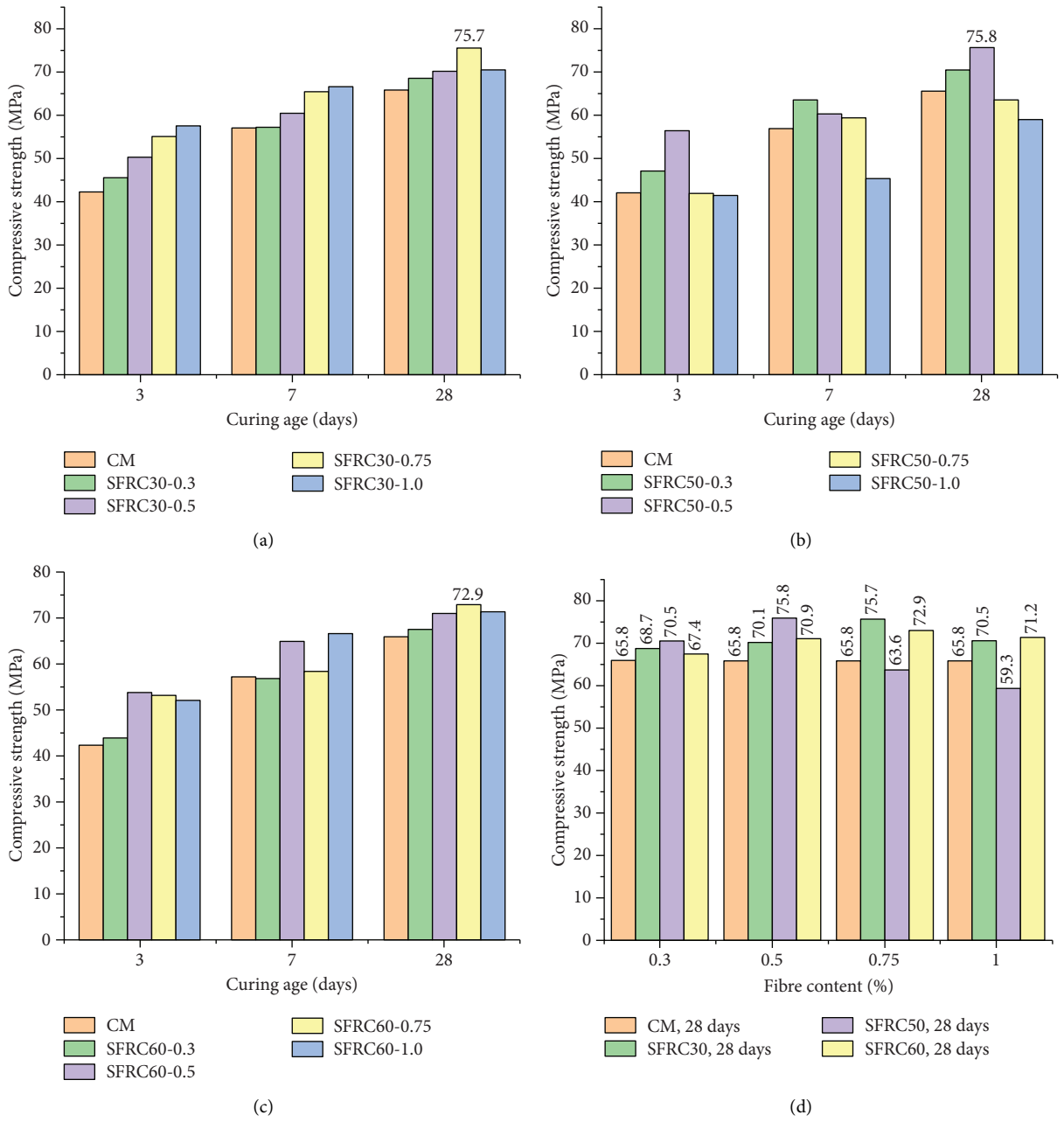

Figure 9: Compressive strength of concrete. (a) Effect of curing age for 30 mm fibre length. (b) Effect of curing age for 50 mm fibre length. (c) Effect of curing age for 60 mm fibre length. (d) Effect of fibre content at 28 days of curing.

to crushing. In addition, the results showed that the small length of fibre requires more fibre content to have the same compressive strength. For example, SFRC50-0.5 had a compressive strength of 75.8 MPa slightly higher than SFRC30-0.75 with a compressive strength of 75.7 MPa. During the crushing of the fibre-reinforced concrete, some sounds were heard, indicating the reorientation of the fibre prior to the ultimate failure of the cube. For SFRC30-0.3, it was noted a difference in compressive strength values between the three tested specimens, i.e., 76.83 MPa, 74.2 MPa, and 55.07 MPa. This is due to the uneven distribution of fibres in the cube, resulting in improper bonding action on the clogged fibres. These findings are in line with the past study by [9]. Concrete with fibre length 50 mm with content more than 0.5% and all specimens of SFRC60 show less compressive strength. This is associated with an increase in weaker zones between the fibre-concrete interface due to the high content and length, which eventually reduces the compressive stiffness of the specimen. During the shrinkage process of concrete, high fibre content could reduce the contact pressure at the fibre-concrete interface that is responsible for the stress transfer. This reduction is associated with the less spacing of fibres in the matrix that reduces the area of concrete surrounding it, hence less imposed pressure after the matrix has shrunken [37].

3.2.2. Splitting Tensile Strength. The results of the tensile strength of concrete are shown in Figure 10. The control mix showed explosive brittle and sudden failure compared to concrete with fibres. The addition of fibres prolongs failure due to the tension-stiffening action of the fibre in the concrete. In this study, the concrete cylinder with fibre showed high resistance after the first crack. The tensile strengths of SFRC60-1.0, SFRC50-0.5, and SFRC50-1.0 were 4.86 MPa, 4.82 MPa, and 4.8 MPa that were 21.5%, 20.5%, and 20% higher than the control mix, respectively. Tensile strength increases as the fibre content increases except for SFRC50-1.0, which showed a slight decrease in strength. The decrease in strength for a long length could be due to the rearrangement of the fibres during casting. The casting processes reduce the angle far less than 90° from the line of splitting force that significantly reduces the effectiveness of load transfer at the interface. The proper orientation of the fibres to the applied load increases the effectiveness of bridging the two halves of the cylinder before they are split [15]. It could also be attributed to the type of fibres used, in which, to some extent, the deformed fibre with the grip for the high fibre content can create microcracks during pulling out of the matrix when the sample is loaded. This increases the likelihood of weaker points along with the fibre-concrete interface, resulting in lower bond strength, and hence lower final tensile strength. The results showed slightly less tensile strength compared to most of the industrial fibres as reported in [38]. This is due to the high temperatures used in the pyrolysis process and the wear of the fibres in the tyre resulting in some defective threads compared to virgin industrial fibres. Although vibration in concrete increases the densification of concrete, internal vibration as compared to external vibration has a negative effect on fibres realignment in the matrix [39]. This is accompanied by segregation of the fibres at a point where the poker vibrator is placed in the matrix, leaving the core part of the sample unreinforced. This effect is greater in small samples, that is, cubes and cylinders, compared to beams. The planned concrete at the core of the specimen loses the ability to withstand more loads as the specimen cracks or crushes due to the high brittleness of high-strength concrete. This resulted in a limited increase in tensile strength for all specimens and low compressive strength for SFRC50-0.75 and 1.0%.

3.2.3. Flexural Strength. The crack pattern, the flexural strength, and the width of the crack of the concrete against the fibre content are plotted in Figures 11 and 12, respectively. Concrete with a fibre length of 50 mm clearly showed the resistance to crack as the content increases. SFRC50-0.3, SFRC50-0.5, SFRC50-0.75, and SFRC50-1.0 had crack widths of 15, 10, 5, and 3 mm, respectively. This indicates the effect of the fibre content to resist crack opening. Concrete with 60 mm fibre length showed superior flexural strength and lesser crack width compared to other mixes with the same fibre content. For example, SFRC60-0.3 had the highest flexural strength of 6 MPa compared to 5 MPa and 5.5 MPa of SFRC 30-0.3 and SFRC50-0.3, respectively. The crack width of SFRC60-0.3 was 9 mm, 47.1% less than SFRC50-0.3, and as the fibre content increases, SFRC60-1.0 showed superior flexural strength values and a very small crack that occurred in line with the point of application of the load. SFRC60-1.0 showed an improvement in strength to 71.1% of the control mix. These results agree with [35]. Large fibre length and high fibre content in concrete have a high-contact area that increases the individual bond forces of fibres in the matrix. This resists the initiation of a plastic hinge after yielding composite in the middle third of the beam span length.

3.2.4. Effect of Fibre on Flexural Toughness and Residual Strength. The load-deflection curves, flexural toughness against fibre content, and residual strength against fibre content are plotted in Figures 13 and 14, respectively. The addition of fibres in the concrete matrix had an effect on flexural load, for example, SFRC30-1.0 had 8, 13.5, 31, and 46.9% high load compared to SFRC30-0.75, SFRC30-0.5, SFRC30-0.3, and CM, respectively. In addition, the long length of the fibre increases the bridging of crack and has a high postbehaviour of the concrete beam. The SFRC60-1.0 had the highest load of 57.4 kN, which is 6.3% and 16% compared to SFRC50-1.0 and SFRC30-1.0, respectively. The beam with high content showed high deflection resulting in high flexural toughness. This is the measure of the energy absorption capacity of concrete, indicating that high fibre content and length in concrete require more load before failure. The SFRC60-1.0 had a superior flexural toughness of 142 Joule; however, the flowability of this concrete is a bit of a challenge. A SFRC60-1.0 beam at deflection equivalent to l/150 had a high residual strength compared to the flexural strength of the control mix; this indicates that its materials can still carry more load without failure. The SFRC60-1.0 and SFRC30-0.3 had residual strengths of 5.6 and 4.23 MPa, in which the control mix had a flexural strength of 4.5 MPa. This remaining strength in concrete indicates the effectiveness of fibre in its structural performance [40]. All these best flexural performances of fibre-reinforced concrete are brought by tension stiffening after the first cracking of the beam leading to strain hardening. Tension stiffening in fibre-reinforced concrete is due to friction stress generated between the fibre and the concrete surfaces, as the fibre tends to pull out from the matrix. This friction stress acts oppositely to the direction of tensile force, in which after the first crack it tends to restore the crack. For long and high content, this action of counteracting the tensile forces in the matrix enhances the postbehaviour of the beam.

3.2.5. Static Modulus and Poisson's Ratio. Young's modulus against fibre content is plotted in Figure 15. The results of this study showed that less fibre content and length had a significant improvement in modulus compared to longer fibre length and content. Concrete with 30 mm length showed a linear increase in Young's modulus from 0.3% to 0.75% fibre content. This increment agrees with [41]. This could be associated with the tendency of the fibre to

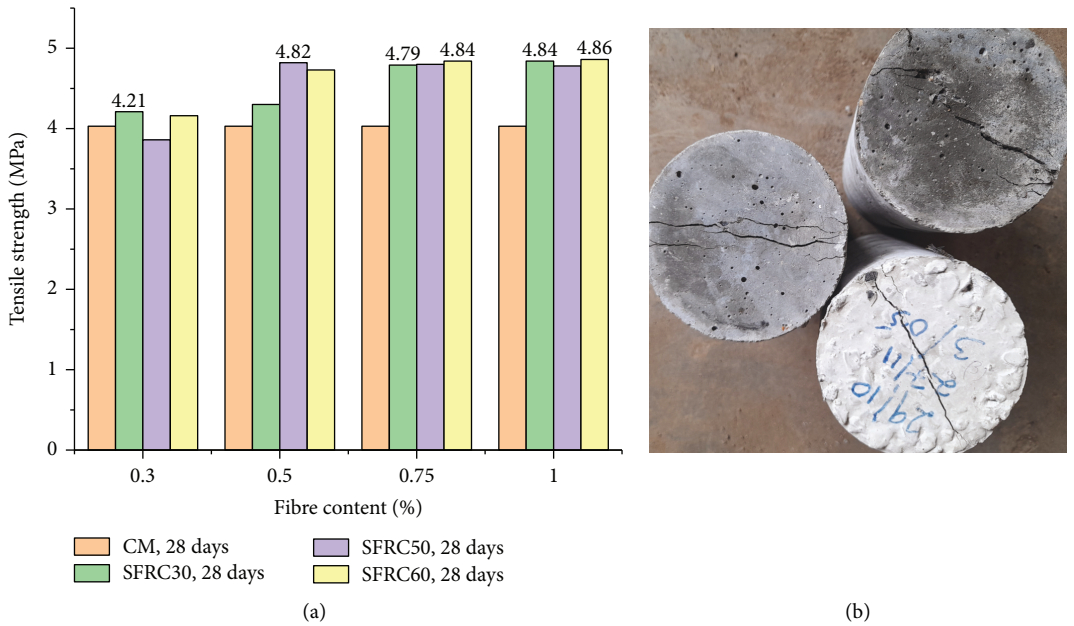

Figure 10: Tensile strength. (a) Effect of fibre length and content on tensile strength of concrete. (b) Failure mode for SFRC50-0.5.

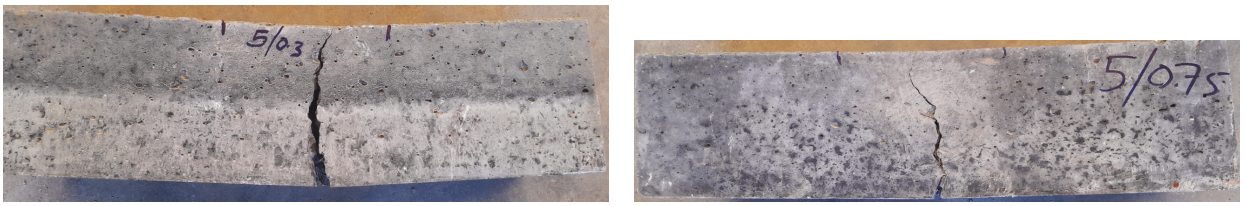

Figure 11: Flexural crack for four-point loads. (a) Crack opening for SFRC50-0.3. (b) Crack opening for SFRC50-0.75.

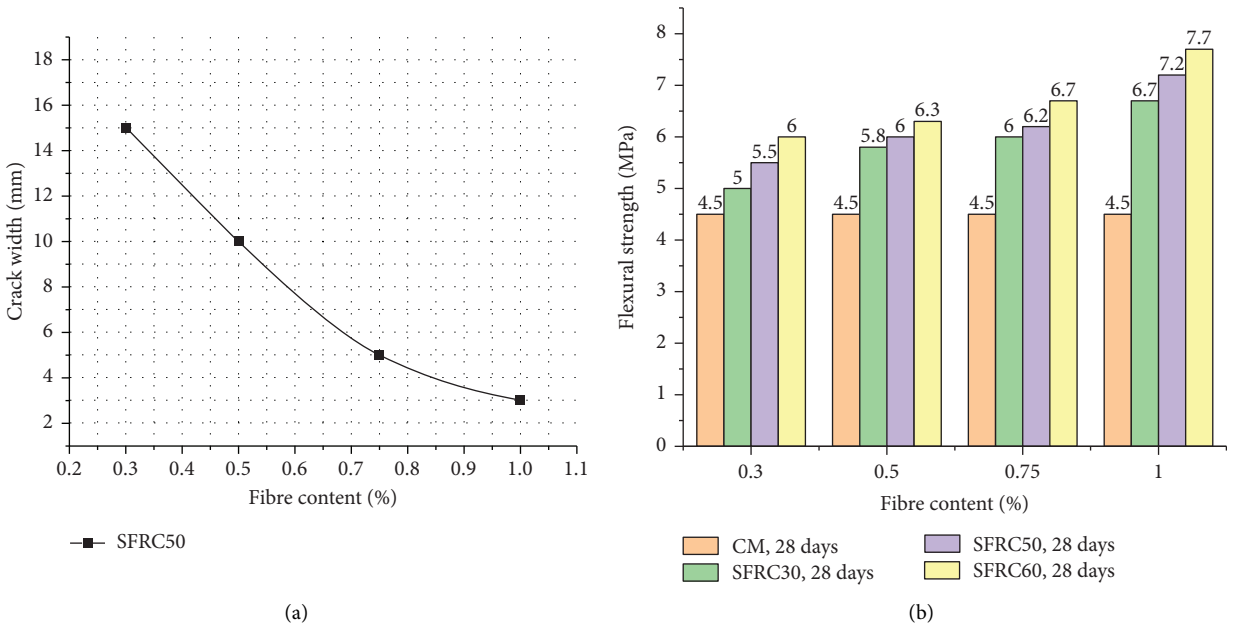

Figure 12: Flexural behaviour of the beam. (a) Effect of fibre content on resisting crack opening. (b) Effect of fibre on flexural strength of concrete.

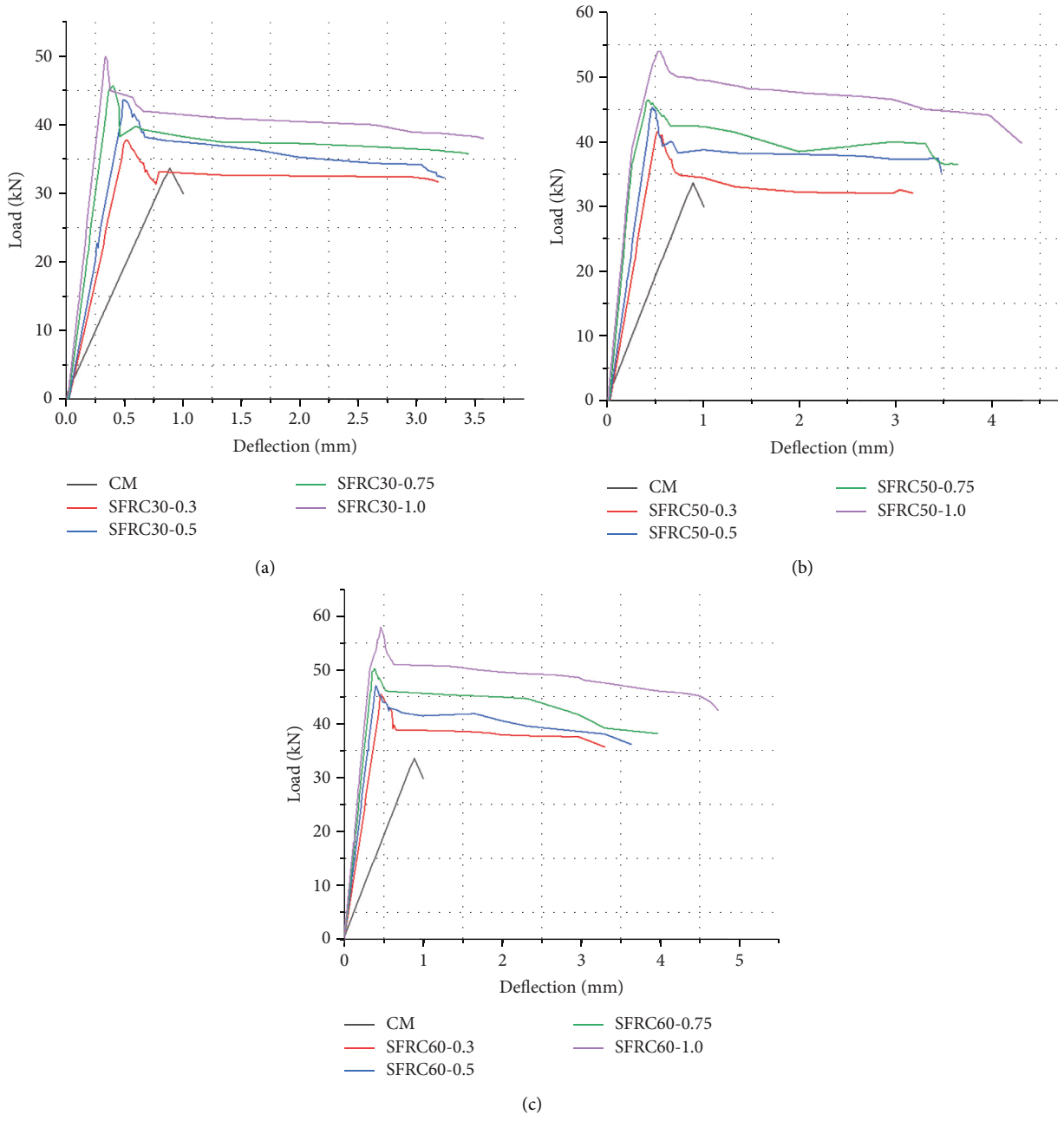

Figure 13: Load-deflection curves. (a) SFRC30. (b) SFRC50. (c) SFRC60.

interlock the aggregates in the matrix and to limit the initiation and propagation of cracks. Concrete with fibre length 50 mm and 0.3% content showed the best improvement on modulus, 35.1% higher than the control mix. This is contrary to [42, 43] that the optimal fibre content is limited to 0.5% only for 30 mm fibre length. These results show that a further increase in fibre length and less content (SFRC50-0.3) could still have a better improvement in modulus. This is attributed to the type of fibre used in the study. It has grips around the fibre that increases the initial friction in the matrix before yielding, but these grips are likely to fail first before the core of the fibre. This early failure of grips increases the number of weaker interfacial transition zones (ITZs) for high content and large fibre lengths. This can lead to a reduction in the compression stiffness of the matrix and therefore a negative effect on Young's modulus. In addition, uneven distribution of fibres could increase the chances of premature failure of concrete matrix as the results showed that there was a sudden drop in modulus for SFRC 50-0.5, SFRC50-1.0, and SFRC 60-0.3. The results showed that, in the absence of an experimental test, the modulus of concrete with waste tyre steel fibres can still be estimated using empirical formulas in various codes of practice. The estimates in ACI308-08 are closer to the experimental results compared to Eurocode 2 for concrete with a fibre length of 30 mm. The control mix showed less modulus compared to the estimated values of

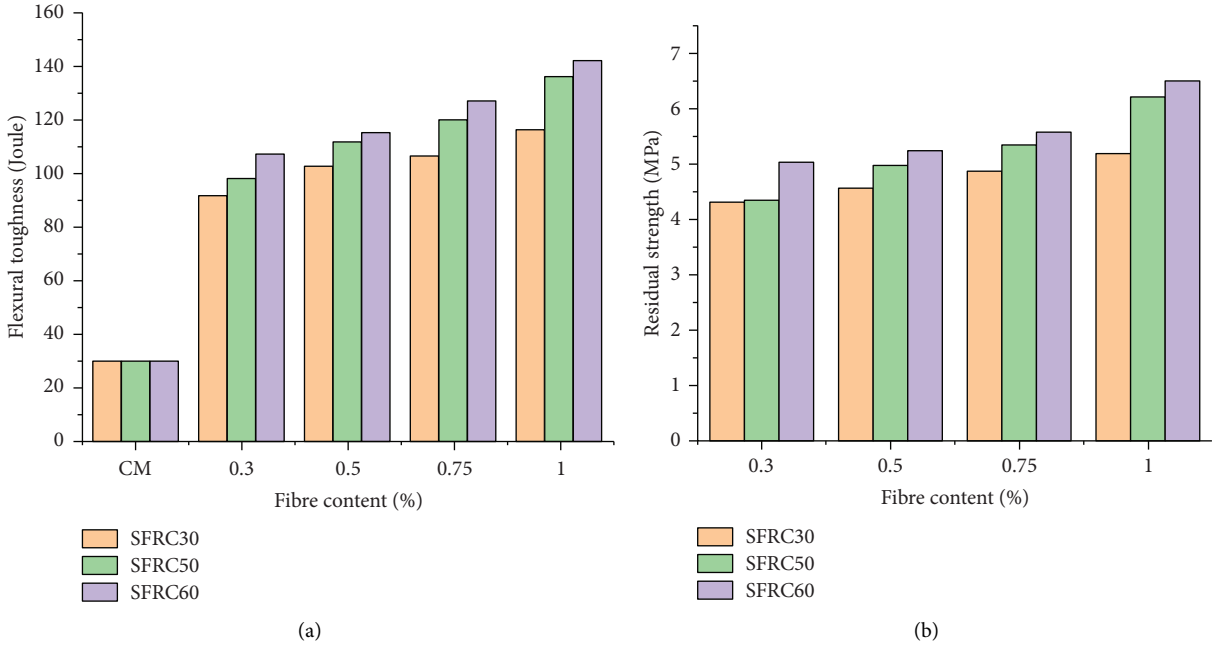

Figure 14: (a) Effect of fibres on flexural toughness. (b) Effect of fibres on residual strength.

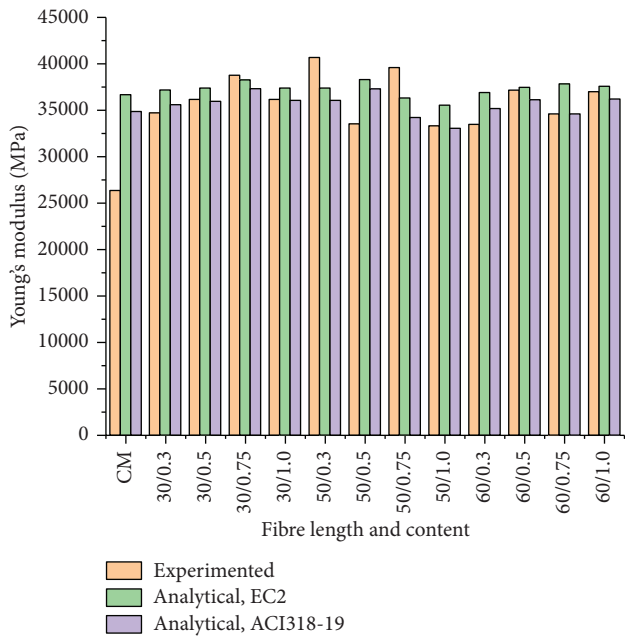

Figure 15: Comparison of the experimental and theoretic Young's modulus of concrete waste from tyres.

the codes. This is due to the sudden crushing of the concrete cylinder that resulted in the highest record of longitudinal strain in the elastic zone, which is taken at 40% of ultimate stress. There is also a bit of divergence of experimental results from these codes. This is due to the unreinforced concrete used in their establishments, in which the resistance to crushing is only due to the aggregates and the binder materials.

The results of Poisson's ratio with longitudinal strain and fibre content are shown in Figure 16. The study showed Poisson's ratio of 0.143 for the control mix that falls within the range of 0.1 to 0.2 for high-performance concrete similar to [44, 45]. This is because HSC without fibre has less elongation in the traverse at a working stress of 40% of the ultimate stress. When the fibres were added, the ductility of HSC increases leading to the bulging of the specimen in the traverse direction leading to high Poisson's ratios of more than 0.143. For instance, SFRC30-0.3 and SFRC50-0.5 had Poisson's ratio of 0.222 and 0.315, being 55.2% and 120.3% higher than control mix, respectively. The HSC with fibres showed many hair cracks before ultimate failure. The dominant failure mode for HSC without fibre and with less fibre content was long longitudinal cracks. In SFRC30, with more content than 0.3%, concrete resists more loads and a high elongation on the longitudinal axis, resulting in a reduction in Poisson's ratio. This decrease in behaviour of Poisson's ratio was also reported in [46]. Concrete with fibre lengths of 50 and 60 mm did not show the best trend as with the fibre length of 30 mm, indicating the complexity of the orientation of large fibre lengths in the matrix. The SFRC50-1.0 had less axial deformation with relatively high lateral deformation resulting in highest Poisson's ratio indicating high ductility of the matrix. Unlike SFRC60, there was high resistance to both axial and lateral deformation due to the high internal lock of the particles in the matrix. This only caused fragmentations on the surface of the sample that is weaker compared to its inner part of the matrix, as shown in Figure 17.

3.3. Durability

3.3.1. Sorptivity. The absorption rate versus fibre content is shown in Figure 18. In this study, a high absorption rate of water was observed for the first six hours, that is, the initial

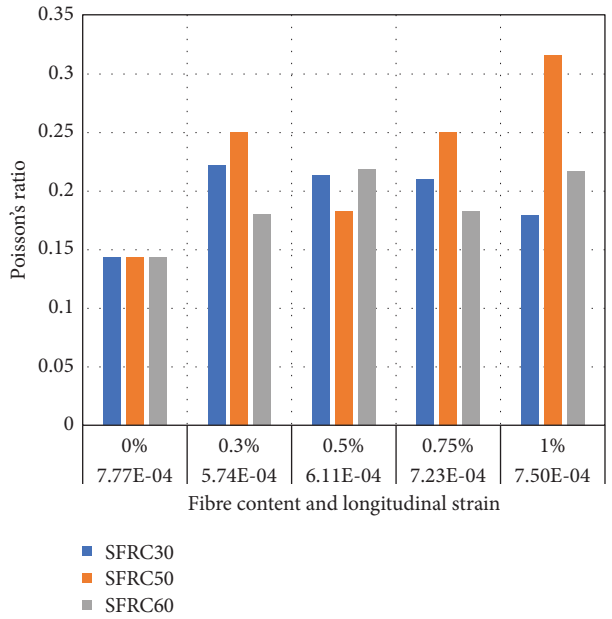

Figure 16: Relationship between longitudinal strain, fibre content, and Poisson's ratio of concrete.

(a) (b)

Figure 17: Failure modes of concrete cylinders under uniaxial compression. (a) SFRC50-1.0. (b) SFR60-0.3.

absorption rate compared to the secondary absorption rate. This is because of the rapid saturation of large pores just at the surface that gradually reduces the infiltration of water with time. Concrete with less fibre content and length, i.e., SFRC30-0.3 showed a bit higher sorptivity coefficients compared to the control mix. This could have been associated with the crowd of fibres on one side of the cube that increases capillaries as a result of close-connected ITZs with less binder. Large lengths with low content properly fill more voids than short fibres with the same content. For instance, SFRC60-0.3 has a sorptivity coefficient of 47.3% less than SFRC30-0.3 due to the long grips in the spiral form available in the selected fibre. This grip breaks the continuity of the fibre-matrix interface, blocks/fills the capillary pores, and reduces internal cracks due to shrinkage during hydration of concrete. This behaviour is consistent with previous studies [16, 47]. It was also observed that an increase in fibre content resulted in an increase in sorptivity coefficient. The SFRC50-1.0 showed a high absorption rate compared to SFRC50-0.5. This was in line with the finding in [48]. More fibres in concrete increase the porosity of concrete leading to rapid capillary rise in the matrix. Furthermore, the results showed the best decrease in the absorption rate of fibre-reinforced concrete (SFRC50-0.5) to 75% of the control mix. This resistance of fibre-reinforced concrete to absorb water increases the durability of the matrix through the inactive

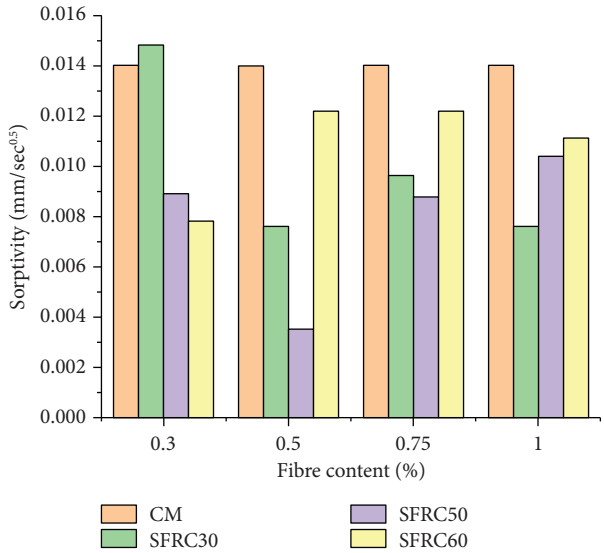

Figure 18: Effect of fibres on the initial sorptivity coefficient of concrete.

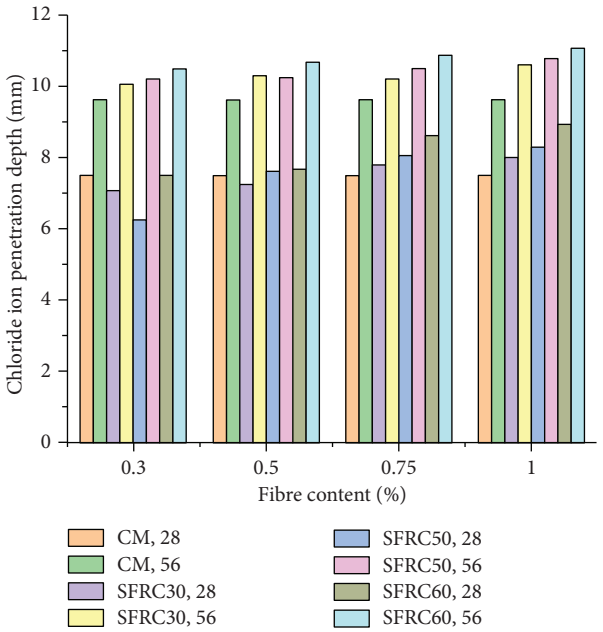

Figure 19: Effect of fibre content on the depth of chloride ion penetration.

process of water ionization by harmful acidic gaseous substances. These gases could ionize water in concrete in the presence of oxygen into hydroxide ions that facilitate the electrochemical process and increase the potential risk of corrosion to the main rebar.

3.3.2. Chloride Ion Penetration. The depth of chlorine ions is plotted in Figure 19. The depth of chloride penetration was initially lower for fibre lengths 30 mm and 50 mm at fibre content of 0.3% to 5.3% and 2.7%, respectively. At 1.0% fibre content, concrete with fibre length of 30 mm showed an increase of chloride ions to 6.7% as in previous study by [43]. With the increase in fibre length and content, the results showed a slight increase in depth of chloride penetration to 18.75% for SFRC60-1.0. This increase in depth is in line with previous findings by [49]. This indicates that increasing the fibre content can increase the diffusion of chloride ions in concrete, not only due to the gradient between internal and external concentrations but also the capillary suction. Suction was more affected by changes in the microstructures of the matrix resulting from the fibres. The results showed that the depth of the chloride ion is less than 20 mm, which is the minimum required concrete cover in structural elements [50]. The use of waste steel fibres in high-strength concrete could have great potential. This could result in less effect of chloride ions to ionize water and initiate the corrosion of conventional steel reinforcement in a structural element.

4. Conclusions and Recommendations

In general, experimental results conclude that the compressive strength of concrete with fibre length of 50 mm and a content of 0.5% is 15.2% higher than control mix. Contrary to some findings in the literature, the synthetic/industrial fibres increase the compressive strength until the fibre content reaches 1.5%. The results of this study have shown the potential for the use of waste tyre steel fibres in concrete production rather than leaving them abandoned in the capitals of developing countries.

The deformed spiral shape of fibre with more content can increase the chances of weaker spots along with the fibre-concrete interface. This could lead to a low bonding strength, resulting in an insignificant improvement in final tensile strength. The concrete beam without fibres (control mix) and all SFRC30 samples have an abrupt flexural failure, but when the length and content increase, the crack is lagged as SFRC50-1.0 has crack width 82.4% smaller compared to SFRC50-0.3. Inclusion of waste tyre fibres in concrete increases Young's modulus of elasticity. The optimal content of waste tyre fibre for the modulus of elasticity was 0.3% for 50 mm fibre length. These fibres in concrete had superior residual strength of 5.68 MPa and flexural toughness of 142 Joule for beam SFRC60-1.0; however, a special mix design is required due to low workability.

The results of this study underline that high-strength concrete with waste tyre steel fibres that can be used in the coastal areas due to the low rate of water absorption with 75% less than the control mix. This indicates the best performance against corrosion attack to the main rebars, although special treatment must be applied to the fibres that protrude on the surface of the concrete. Although this study showed performance in compressive strength at 0.5% of the fibre content and 50 mm fibre length, nothing has been examined for the fibre content between 0 and 0.3%, 0.3–0.5%, 0.5–0.75%, and 0.75–1.0%. In addition, the durability test was not performed for more than 56 days. In the future, research is recommended to evaluate the mechanical properties and attachment behaviour of the fibre-concrete interface at high temperatures.

Data Availability

The data used to support the findings of this study are included in the article.

Conflicts of Interest

The authors declare that they have no conflicts of interest.

Authors' Contributions

Daudi S. Augustino contributed to conceptualization, methodology, validation, formal analysis, investigation, resources, original draft writing, review and editing, and visualization. Richard O. Onchiri contributed to supervision and reviewing. Charles Kabubo contributed to supervision and reviewing. Christopher Kanali contributed to supervision and reviewing.

References

[1] C. Bu, D. Zhu, L. Liu et al., "A study on the mechanical properties and Microcosmic mechanism of Basalt fiber Modified rubber Ceramsite concrete," *Buildings*, vol. 12, no. 2, p. 103, 2022.

[2] J. H. A. Rocha, F. P. Galarza, N. G. C. Chileno et al., "Compressive strength Assessment of Soil-cement blocks incorporated with waste Tire steel fiber," *Materials*, vol. 15, no. 5, p. 1777, 2022.

[3] K. Pilakoutas, M. Guadagnini, K. Neocleous, and S. Matthys, "Design guidelines for FRP reinforced concrete structures," *Proceedings of the Institution of Civil Engineers - Structures and Buildings*, vol. 164, no. 4, pp. 255–263, 2011.

[4] A. Padanattil, J. Karingamanna, and M. K.M., "Novel hybrid composites based on glass and sisal fiber for retrofitting of reinforced concrete structures," *Construction and Building Materials*, vol. 133, pp. 146–153, 2017.

[5] K. Olsson and O. Dahlblom, *Structural Mechanics Modelling and Analysis of Frames and Trusses*, John Wiley & Sons, UK, 2016.

[6] Y. Zhang, L. Chen, and D.-L. Zhou, "Dynamic Mechanical Properties of Hybrid Fiber Reinforced concrete," *International Journal of Protective Structures*, 2022.

[7] C. B. Demakos, C. C. Repapis, and D. P. Drivas, "Experimental investigation of shear strength for steel fibre reinforced concrete beams," *The Open Construction & Building Technology Journal*, vol. 15, no. 1, pp. 81–92, 2021.

[8] T.-F. Yuan, D.-Y. Yoo, J.-M. Yang, and Y.-S. Yoon, "Shear capacity contribution of steel fiber reinforced high-strength concrete compared with and without Stirrup," *International Journal of Concrete Structures and Materials*, vol. 14, no. 1, 2020.

[9] L. Zhang, J. Zhao, C. Fan, and Z. Wang, "Effect of surface shape and content of steel fiber on mechanical properties of concrete," *Advances in Civil Engineering*, vol. 2020, Article ID 8834507, 11 pages, 2020.

[10] W. Kaufmann, A. Amin, A. Beck, and M. Lee, "Shear transfer across cracks in steel fibre reinforced concrete," *Engineering Structures*, vol. 186, pp. 508–524, 2019.

[11] D. Salim, H. Mohammed, A. Abdulazeez, and A.-H. Asaad, "Flexural strength and ductility of ultra high-performance cement-based composites (UHP-CC)," *Journal of Applied Engineering Science*, vol. 20, no. 1, pp. 131–136, 2022.

[12] P. J. van der Aa, "Biaxial Stresses in Steel Fibre Reinforced Concrete Modelling the Pull-Out Behaviour of a Single Steel Fibre Using FEM," *Masters Thesis, Eindhoven University of Technology*, vol. 1, 2014.

[13] Y. Zhan and G. Meschke, "Analytical Model for the Pullout behavior of straight and hooked-end steel fibers," *Journal of Engineering Mechanics*, vol. 140, no. 12, Article ID 04014091, 2014.

[14] B. Ali, L. A. Qureshi, and R. Kurda, "Environmental and economic benefits of steel, glass, and polypropylene fiber reinforced cement composite application in jointed plain concrete pavement," *Composites Communications*, vol. 22, Article ID 100437, 2020.

[15] J. Du, W. Meng, K. H. Khayat et al., "New development of ultra-high-performance concrete (UHPC)," *Composites Part B: Engineering*, vol. 224, Article ID 109220, 2021.

[16] S. Yuvraj, S. Sukhwant, and S. Harvinder, "Effect of Steel Fibers on the Sorptivity of Concrete," *Fatigue, Durability, and Fracture Mechanics*, Springer, Singapore, 2019.

[17] EN 197-1, *Cement - Part 1: Composition, Specifications and Conformity Criteria for Common Cements Ciment*, pp. 1–29, European Standard, Latin; Greek; Cyrillic, 2000.

[18] ASTM C33, *Standard Specification for Concrete Aggregates*, pp. 1–11, ASTM, West Conshohocken, Pennsylvania, 2013.

[19] BS 812-2, "Testing of Aggregates," *Method of Determination of Density*, pp. 1–22, British Standard, Citi Lights Tower, Vivekananda, 1995.

[20] CML, "Laboratory Testing Manual, Central Materials Laboratory," *Testing Manual, Ministry of Works*, pp. 1–320, Tanzania, 2000.

[21] ASTM A820, *Standard Specification for Steel Fibers for Fiber-Reinforced Concrete*, ASTM, West Conshohocken, Pennsylvania, 2011.

[22] J. C. Ndayambaje, "Structural Performance and Impact Resistance of Rubberized concrete," *ASTM International*, vol. 5, no. 1, 2018.

[23] R. Serafini, L. M. Mendes, R. P. Salvador, and A. D. de Figueiredo, "The Effect of Elevated Temperatures on the Properties of Cold-Drawn Steel Fibres," *Magazine of Concrete Research*, vol. 73, no. 18, pp. 936–944, 2021.

[24] N. Siraj, A. Dinku, and N. S. Kedir, "Synthesis and characterization OF PYROLISED RECYCLED steel FIBERS for use IN reinforced concrete," *International Journal OF Engineering Sciences & Management Research*, vol. 4, no. 6, 2017.

[25] ACI 211, "Ide for selecting proportions for high-strength concrete using Portland cement and other cementitious materials," *ACI*, vol. 211, pp. 1–25, 2008.

[26] L. W. Katimbi, *The Effect of Retarding Chemical Superplasticizers on the Setting Time of Cement Pastes in Kenya: A Case Study of Ready Mix Concrete*, University of Nairobi, Nairobi, Kenya, 2017.

[27] M. Benaicha, A. Hafidi Alaoui, O. Jalbaud, and Y. Burtschell, "Dosage effect of superplasticizer on self-compacting concrete: Correlation between rheology and strength," *Journal of Materials Research and Technology*, vol. 8, no. 2, pp. 2063–2069, 2019.

[28] EN 12390, *Testing Hardened Concrete: Part 3: Compressive Strength of Test Specimens*, European standard, European, 2001.

[29] B. S. En 12390, "Testing hardened concrete. Part 6: tensile splitting strength of test specimens," *British standard*, vol. 3, no. 1, p. 10, 2000.

[30] ASTM C1018, *Standard Test Method for Flexural Toughness and First-Crack Strength of Fiber-Reinforced Concrete (Using*

Beam With Third-Point Loading), ASTM, West Conshohocken, Pennsylvania, 1997.
[31] ASTM C1609, *Standard Test Method for Flexural Performance of Fiber-Reinforced concrete (Using Beam with Third-Oint Loading)*, ASTM, West Conshohocken, Pennsylvania, 2010.
[32] ASTM C469, *Standard Test Method for Static Modulus of Elasticity and Poisson's Ratio of Concrete in Compression*, pp. 2–6, ASTM, West Conshohocken, Pennsylvania, 2010.
[33] ASTM C1585, *Standard Test Method for Measurement of Rate of Absorption of Water by Hydraulic-Cement Concretes*, West Conshohocken, Pennsylvania, 2013.
[34] ASTM C1543, "Standard test Mthod for Determining the Penetration of Chloride Ion into Concrete by Ponding," ASTM, West Conshohocken, Pennsylvania, 2010.
[35] X. Yan, Y. Gao, Y. Luo, Y. Bi, and Y. Xie, "Effect of different steel fiber types on mechanical properties of ultra-high performance concrete," *IOP Conference Series: Materials Science and Engineering*, vol. 1167, no. 1, Article ID 012001, 2021.
[36] M. Chen, H. Si, X. Fan, Y. Xuan, and M. Zhang, "Dynamic compressive behaviour of recycled tyre steel fibre reinforced concrete," *Construction and Building Materials*, vol. 316, Article ID 125896, 2022.
[37] P. S. Mangat and M. M. Azari, "A Theory for the Free Shrinkage of Steel Fibre Reinforced Cement Matrices," *Journal of Materials Science volume*, vol. 19, 1984.
[38] B. Ali, R. Kurda, H. Ahmed, and R. Alyousef, "Effect of recycled tyre steel fiber on flexural toughness, residual strength, and chloride permeability of high-performance concrete (HPC)," *Journal of Sustainable Cement-Based Materials*, pp. 1–17, 2022.
[39] L. Li, "Fibre Distribution Characterization and its Impact on Mechanical Properties of Ultra-high Performance Fibre Reinforced Concrete," *Materials*, vol. 13, no. 22, 2019.
[40] A. Michalik, F. Chyliński, J. Bobrowicz, and W. Pichór, "Effectiveness of concrete reinforcement with recycled tyre steel fibres," *Materials*, vol. 15, no. 7, p. 2444, 2020.
[41] P. Shanmugam and S. Gopalan, "Effect of fibers on strength and elastic properties of bagasse ash blended HPC composites," *Journal of Testing and Evaluation*, vol. 48, no. 2, Article ID 20170698, 2020.
[42] B. Ali, R. Kurda, B. Herki et al., "Effect of varying steel fiber content on strength and permeability characteristics of high strength concrete with micro silica," *Materials*, vol. 13, no. 24, pp. 5739–5817, 2020.
[43] B. Ali, E. Yilmaz, A. R. Tahir, F. Gamaoun, M. H. el Ouni, and S. M. Murtaza Rizvi, "The durability of high-strength concrete containing waste Tire steel fiber and coal fly ash," *Advances in Materials Science and Engineering*, vol. 2021, Article ID 7329685, 19 pages, 2021.
[44] B. Persson, "Poisson's Ratio of High-Performance concrete," *Cement and Concrete Research*, vol. 29, 1999.
[45] A. S. Carey, M. N. McBride, Y. Hammi et al., "Stress-strain behaviour and failure properties of ultra-high-performance concrete," *Institution of Civil Engineers - Construction Materials*, vol. 1, pp. 1–12, 2020.
[46] A. A. Okeola, S. O. Abuodha, and J. Mwero, "The effect of specimen shape on the mechanical properties of sisal fiber-reinforced concrete," *The Open Civil Engineering Journal*, vol. 12, no. 1, pp. 368–382, 2018.
[47] D. Vafaei, R. Hassanli, X. Ma, J. Duan, and Y. Zhuge, "Sorptivity and mechanical properties of fiber-reinforced concrete made with seawater and dredged sea-sand," *Construction and Building Materials*, vol. 270, Article ID 121436, 2021.
[48] T. Akhtar, B. Ali, N. Ben Kahla et al., "Experimental investigation of eco-friendly high strength fiber-reinforced concrete developed with combined incorporation of tyre-steel fiber and fly ash," *Construction and Building Materials*, vol. 314, Article ID 125626, 2022.
[49] W. Chen, H. Zhu, Z. He, L. Yang, L. Zhao, and C. Wen, "Experimental investigation on chloride-ion penetration resistance of slag containing fiber-reinforced concrete under drying-wetting cycles," *Construction and Building Materials*, vol. 274, Article ID 121829, 2021.
[50] BS 8110-1, *Structural Use of concrete. Part 1: Code of Practice for Design & Construction*, Citi Lights Tower, Vivekananda, 1997.